

SCIENTIFIC REPORTS

OPEN

Sperm physiology varies according to ultradian and infradian rhythms

Ayelén Moreno-Irusta^{1,2}, Jackelyn M. Kembro², Esteban M. Domínguez^{1,2}, Arturo Matamoros-Volante³, María N. Gallea^{1,2}, Rosa Molina⁴, Hector A. Guidobaldi^{1,2}, Claudia L. Treviño³, María J. Figueras^{1,2}, Ana Babini⁵, Nelso A. Paina⁶, Carlos A. N. Mercado⁶ & Laura C. Giojalas^{1,2}

Received: 17 September 2018

Accepted: 1 April 2019

Published online: 12 April 2019

The spermatozoon must be physiologically prepared to fertilize the egg, process called capacitation. Human sperm samples are heterogeneous in their ability to capacitate themselves, which leads to variability between samples from the same or different donors, and even along the seasons. Here we studied sperm variation in the capacitation state according to the ability of capacitated spermatozoa to acrosome react upon stimulation (%ARi) and to be recruited by chemotaxis (%Chex). Both indirect indicators of sperm capacitation increased along the incubation time with fluctuations. Those capacitated sperm recruited by chemotaxis showed an ultradian rhythm with a cycle every 2 h, which might be influenced by unknown intrinsic sperm factors. Two infradian rhythms of 12 months for the %ARi and of 6 months for %Chex were observed, which are associated with the joint action of temperature and photoperiod. Thus, to avoid false negative results, human sperm samples are recommended to be incubated for a long period (e.g. 18 h) preferably in spring time. This innovative point of view would lead to better comprehend human reproductive biology and to think experimental designs in the light of sperm cyclicity or to improve sperm aptitude for clinical purposes.

The spermatozoon must be in such a physiological state to guarantee not only fertilization but also early embryo development¹. This physiological preparation is acquired after a period of incubation under adequate physical and chemical conditions. This process is generally known as sperm capacitation^{2,3}, comprising a series of biochemical and biophysical changes occurring at the sperm plasma membrane and also inside the cell. For instance, during capacitation, changes have been reported such as an increase in intracellular pH^{4,5}, calcium⁶, reactive oxygen species (ROS)⁷, cAMP and protein tyrosine phosphorylation⁸. Once the spermatozoon is capacitated, it can undergo several sperm processes that help successful fertilization, such as the induced acrosome reaction⁹ and the orientation of its movement by following the concentration gradient of an attractant molecule, known as chemotaxis^{10,11}.

The timing and incubation conditions for sperm capacitation vary according to the species, but also between laboratories. In the case of human spermatozoa, even though most researchers include the essential components to support capacitation in the culture medium (calcium, bicarbonate and albumin)¹², the timing differs greatly between labs, from two hours to overnight incubation. There is also great variation between semen samples from the same and different donors¹³. Human sperm variations may be attributed, among other factors, to a seasonal change in climate, especially in regions with marked seasonality, but such reports are controversial. While some groups reported variation in spermogram parameters during the year^{14–18} others did not observe any seasonal trends^{19–21}. These differences could be due to sample size and method of analysis. Moreover, it is worth noting that most of the semen parameters analyzed (i.e. sperm concentration, motility and morphology) are still controversial as predictors of male fertility. Parameters more representative of the global physiological state would be preferable, for example sperm capacitation^{22,23}. To verify whether sperm capacitation varies with some kind of periodicity, e.g., less than 24 h (ultradian rhythm) or higher than 24 hours (infradian rhythm, which includes

¹Universidad Nacional de Córdoba (UNC), Facultad de Ciencias Exactas, Físicas y Naturales, Centro de Biología Celular y Molecular, Córdoba, Argentina. ²Instituto de Investigaciones Biológicas y Tecnológicas, UNC, CONICET, FCEFYN, Córdoba, Argentina. ³Departamento de Genética del Desarrollo y Fisiología Molecular, Instituto de Biotecnología, Universidad Nacional Autónoma de México, Cuernavaca, Mexico. ⁴Laboratorio de Andrología y Reproducción (LAR), Córdoba, Argentina. ⁵Universidad Nacional de Córdoba, Facultad de Ciencias Médicas, Instituto Universitario de Medicina Reproductiva (UMER), Córdoba, Argentina. ⁶Universidad Nacional de Córdoba, Hospital Universitario de Maternidad Nacional, Córdoba, Argentina. Correspondence and requests for materials should be addressed to L.C.G. (email: lgiojalas@unc.edu.ar)

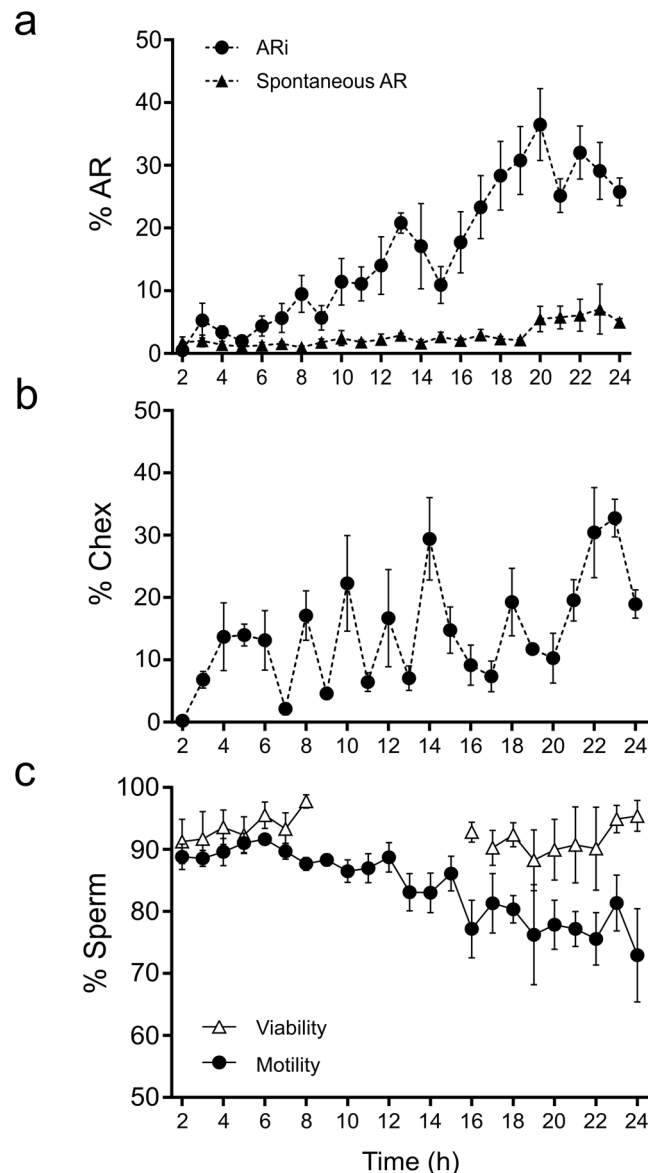


Figure 1. Sperm physiology fluctuation along incubation time. Percentage of AR_i spermatozoa (circles) and the percentage of spontaneous AR spermatozoa (triangles) during 24-hours incubation period under capacitating conditions (a). Percentage of Chex during 24-hours incubation period under capacitating conditions (b). Percentage of motile (black circles) and live (white triangles) spermatozoa, during 24 hours incubation under capacitating conditions (c). AR_i, induced acrosome reaction; Chex, capacitated spermatozoa recruited by chemotaxis. Data are expressed as the mean \pm SEM, of 8 independent samples.

periods of one year, i.e. a circannual rhythm), robust mathematical approaches should be applied as those used to determine cyclicity in epidemiological events²⁴.

Since our laboratory is in the city of Córdoba (Argentina), which is immersed in a humid subtropical climate with marked seasonality, we investigated whether sperm capacitation varies according to an ultradian and/or infradian rhythm, with the aim of explaining sperm physiology variations.

Results

Sperm physiology ultradian variation. We first evaluated the temporal dynamics of the capacitation state in the same sperm sample, every hour, during 24 h incubation, by means of the % AR_i¹² and % Chex spermatozoa²⁵.

The mean % AR_i (Fig. 1a) and % Chex spermatozoa (Fig. 1b) gradually increased with fluctuations as a function of incubation time. Interestingly, the percentage of sperm samples showing a defined range of capacitation (either AR_i or Chex) also varied during incubation. For both parameters, 100% of the semen samples showed a value lower than 3% after 2 h incubation, in contrast to the 70–100% of the samples that achieved a value greater than 10% after 18 h incubation (Fig. 2).

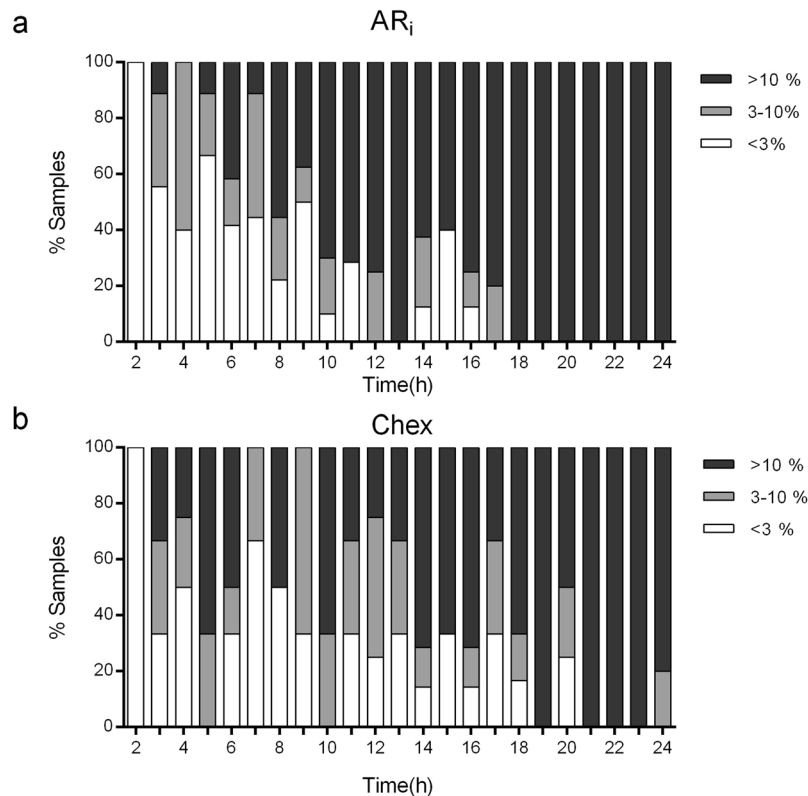


Figure 2. Distribution of sperm samples according to the physiological state. Percentage of samples showing a defined range of % AR_i (a) or % Chex (b), determined during incubation. The corresponding ranges of each parameter are shown in the upper right corner of each Figure. AR_i , induced acrosome reaction; Chex, capacitated spermatozoa recruited by chemotaxis. Data include measurements of 9 independent experiments performed with ejaculates from different donors.

In addition, the intracellular calcium and the hyperpolarization of the sperm membrane (parameters associated with sperm capacitation) apparently increased during incubation compared with non-capacitated spermatozoa (Fig. 3). Moreover, the increase in sperm capacitation over time was verified by protein tyrosine phosphorylation (Supplementary Fig. S1). As expected, the spontaneous AR (Fig. 1a), and sperm motility and viability (Fig. 1c) remained quite stable throughout incubation.

The occurrence of peaks and valleys in the % AR_i and % Chex spermatozoa was also observed in individual samples (Supplementary Fig. S2). Therefore, the fluctuations observed may be due to a random phenomenon or to sperm capacitation periodicity (i.e., peaks recurring at a certain time lag). To elucidate the nature of the variation, we studied the presence of ultradian rhythms (less than 24 h) by autocorrelation analysis of time series. The % AR_i spermatozoa showed an exponential decay in the autocorrelation function for lags up to 4 h (Fig. 4a), indicating that variations in AR_i may represent a stochastic process with short-range correlations. In contrast, the mean % Chex spermatozoa showed a cyclic fluctuation with peaks and valleys, with a period of approximately 2 h (Fig. 4b), as shown by the periodic behavior observed in the autocorrelation function, with negative values followed by positive values at an interval of 2 h (Fig. 4b). This cyclic behavior was also seen in individual sperm samples (Fig. 4b; Supplementary Fig. S2). Our results indicate that both parameters increase with time, and that only the % Chex spermatozoa fluctuate with an ultradian rhythm with a 2-hour cycle.

Sperm physiology infradian variation. We next studied whether conventional semen parameters (concentration, morphology and motility) vary or not over the seasons. The three parameters, provided by a local andrology lab, seem to behave quite stable throughout the year, except for a decrease in sperm count in summer time in two of the three years (Fig. 5). However, since the autocorrelation coefficient approached zero, seasonal periodicity is not evident, (Supplementary Fig. S3); hence, we next looked for seasonality in sperm capacitation. The percentages of AR_i and Chex spermatozoa were determined in the middle of each month, and the cells incubated under capacitating conditions for 4 h (incubation time chosen by many scientists) and 18 h (time at which most of the samples show a capacitation level higher than 10% in this study), during three consecutive years (from 2014 to 2016). From visual observation of the time series of % AR_i and % Chex after 18 h of incubation, an apparent infradian variation over the years is observed (solid line in Fig. 6a,b). Moreover, for both sperm parameters, the three year mean value for peaks was significantly higher than that observed in valleys (% AR_i : $46 \pm 6\%$ vs $12 \pm 3\%$; $p < 0,001$; % Chex: $12 \pm 2\%$ vs $5 \pm 1\%$; $p < 0.0002$). A similar behavior was observed after 4 h of incubation (solid line in Supplementary Fig. S4). To verify the existence of a circannual variation, an in-depth mathematical analysis was performed. Thus, the autocorrelation analysis for the % AR_i showed negative values at

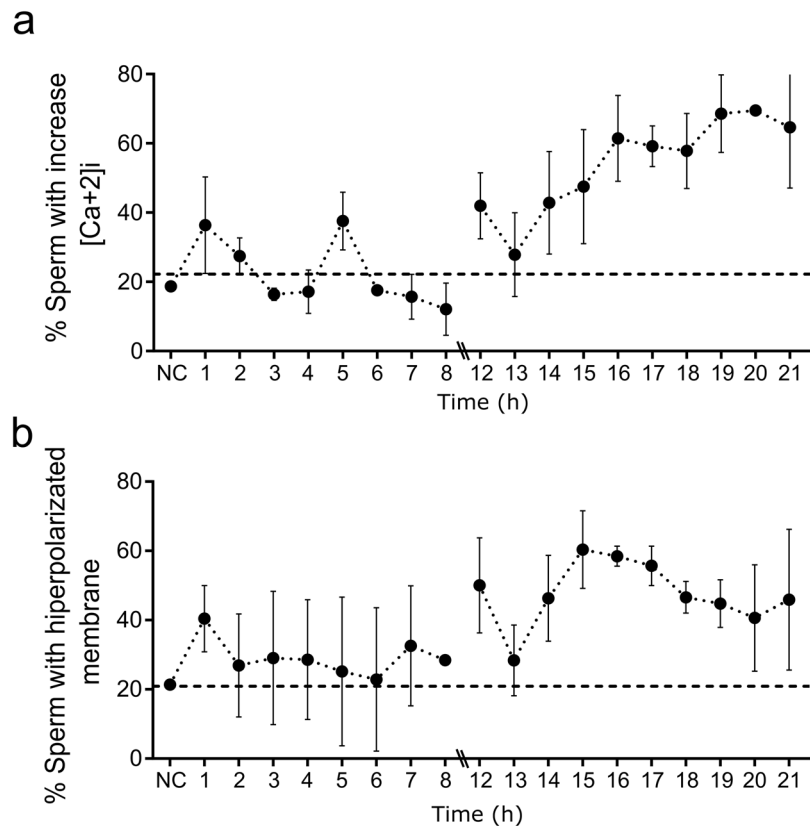


Figure 3. Sperm membrane potential and intracellular Ca²⁺ along incubation time. Percentage of spermatozoa showing an increase in: the intracellular calcium (a) and the hyperpolarized membrane (b). For the analysis, the percentage of spermatozoa exceeding the third quartile of fluorescence intensity was taken; the dotted line shows the percentage of spermatozoa that exceeds the third quartile in non-capacitated samples (NC). Data are expressed as the mean ± SEM of 8 independent experiments performed with ejaculates from different donors.

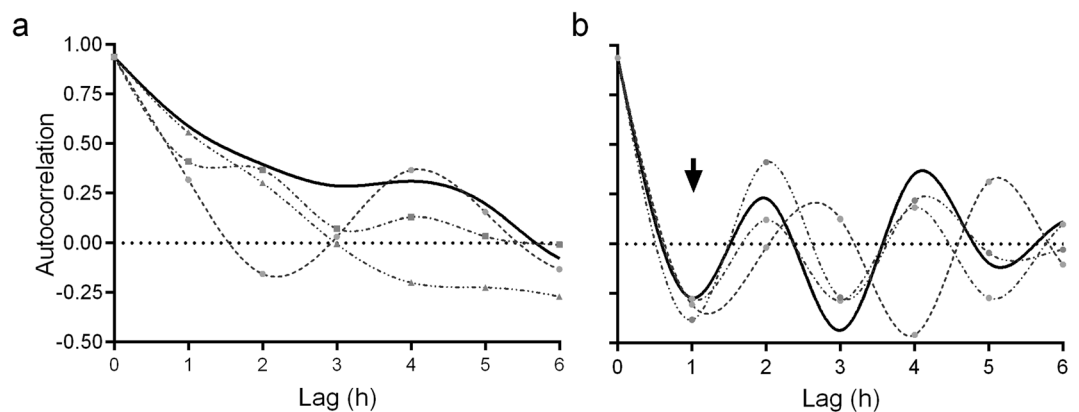


Figure 4. Verification of cyclicality in sperm physiology along incubation time. Autocorrelation analysis of time series of three representative samples (gray lines) and the average of all the samples (N = 7; black line) from data represented in Fig. 1, determined as: % AR_i, (a) and % Chex (b) during 24-hours incubation period. Black arrow points to a negative autocorrelation value (average curve) that is followed by a positive one, indicating that overall at 1-hour intervals higher values are followed by lower values, while the lower are followed by larger values, indicating the existence of periodicity. ARI, induced acrosome reaction; Chex, capacitated spermatozoa recruited by chemotaxis.

6 months followed by positive values at 12 months, reflecting variations for periods of one year (Fig. 7a). A similar result was obtained with the Wavelet analysis run at different time scales. We found that the scale of 12 months shows periodicity according to the variations observed in the alternation of red (high cwt) and blue (low cwt) patterns (Supplementary Fig. S5) where the corresponding wavelet coefficients are shown as peaks and valleys

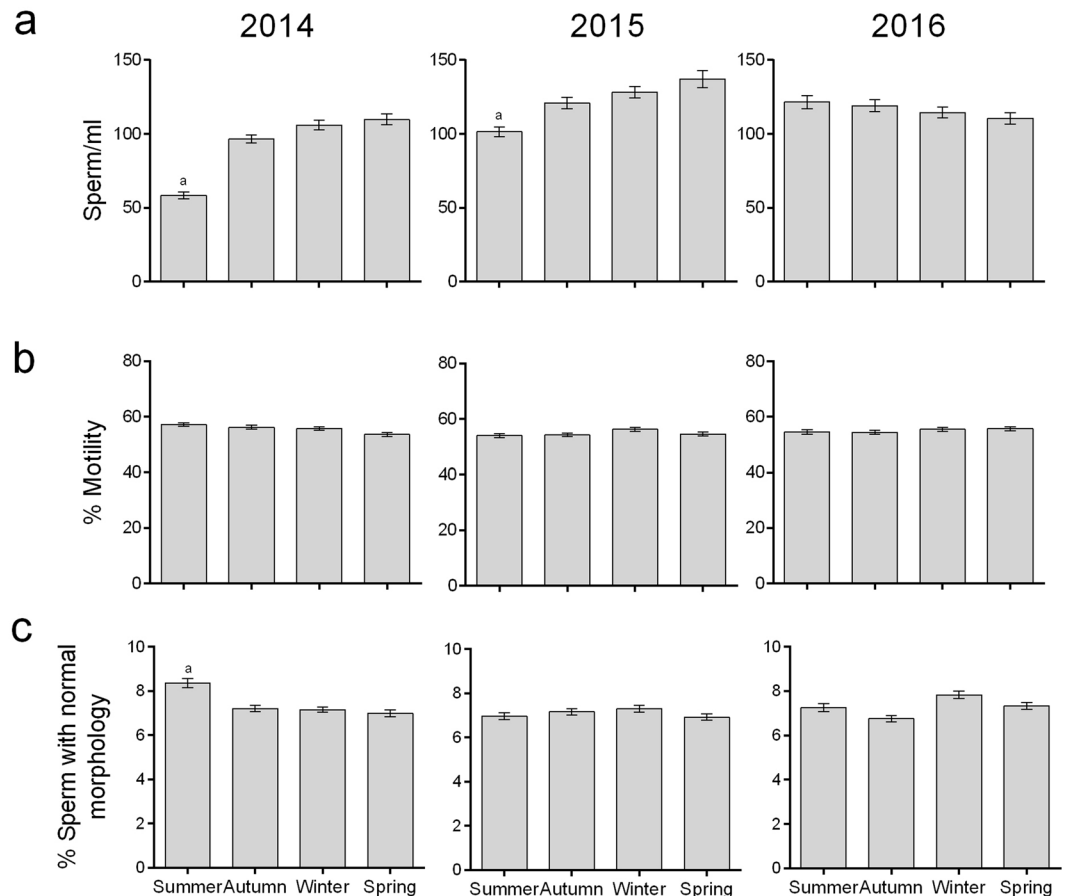


Figure 5. Sperm concentration, motility and morphology values along a three-year period (2014–2016). Sperm concentration (a). Percentage of motile sperm (b). Percentage of spermatozoa with normal morphology (c). Data are expressed as the mean \pm SEM of $N \sim 1400$ samples per year. ^aStatistically significant differences vs all the other categories.

in Fig. 6 (dotted lines), hence, % AR_i varies with a circannual rhythm with a peak in spring time. These results were further verified by the complex Gaussian wavelet (Supplementary Fig. S5). Even though the level of Chex seems also to vary along the year, its periodicity is apparently different from that shown by the AR_i (Fig. 7b). Thus, the three periodicity tests showed an infradian cycle that is repeated every 6 months, with peaks in autumn and spring (Figs 6b and 7b, Supplementary Fig. S5).

In addition, we mathematically verified the yearly variations of temperature and photoperiod, parameters that govern seasonality in our region. As expected, the autocorrelation and Wavelet analysis show a circannual periodicity in these parameters (Figs 6c and 7c, Supplementary Fig. S5). We next investigated whether the periodicity of these meteorological parameters was correlated with those linked to sperm capacitation. High levels of correlations are observed between the Wavelet coefficients of the AR_i and meteorological parameters. Thus, the peak of % AR_i precedes in 1 or 2 month those of photoperiod and temperature, respectively (inset Fig. 6c). It is worth to note that a similar correlation analysis cannot be performed between % Chex and meteorological parameters since they do not share the same periodicity. These results show the existence of seasonal variation in the sperm capacitation state, at least as indirectly evaluated as the percentages of AR_i and Chex spermatozoa.

Discussion

Here we show that sperm physiology varies with different rhythms observed at different time scales: ultradian (a 2 h cycle for % Chex sperm) and infradian (a 6-months cycle for % Chex sperm and a 12-month cycle for % AR_i sperm).

Both indicators of sperm capacitation increase along time with a fluctuating pattern of peaks and valleys. The % AR_i showed no periodicity, while the % Chex expressed a well-defined cycle of approximately 2 hours, consistent with the notion that the capacitation state is transient and lasts for 2 hours^{26,27}. The different behavior of these two parameters may reflect technical influence, since it is probable that post-capacitated spermatozoa (those that lost the capacitation state) also acrosome react upon pharmacological induction^{28,29}, while only capacitated acrosome-intact spermatozoa are able to respond to a chemoattractant stimulus^{11,30,31}. It is worth noting that high levels of motility and viability are observed throughout the 24-hour incubation period, suggesting that the observed variations are preferably associated to changes in the capacitation state. In addition, other parameters

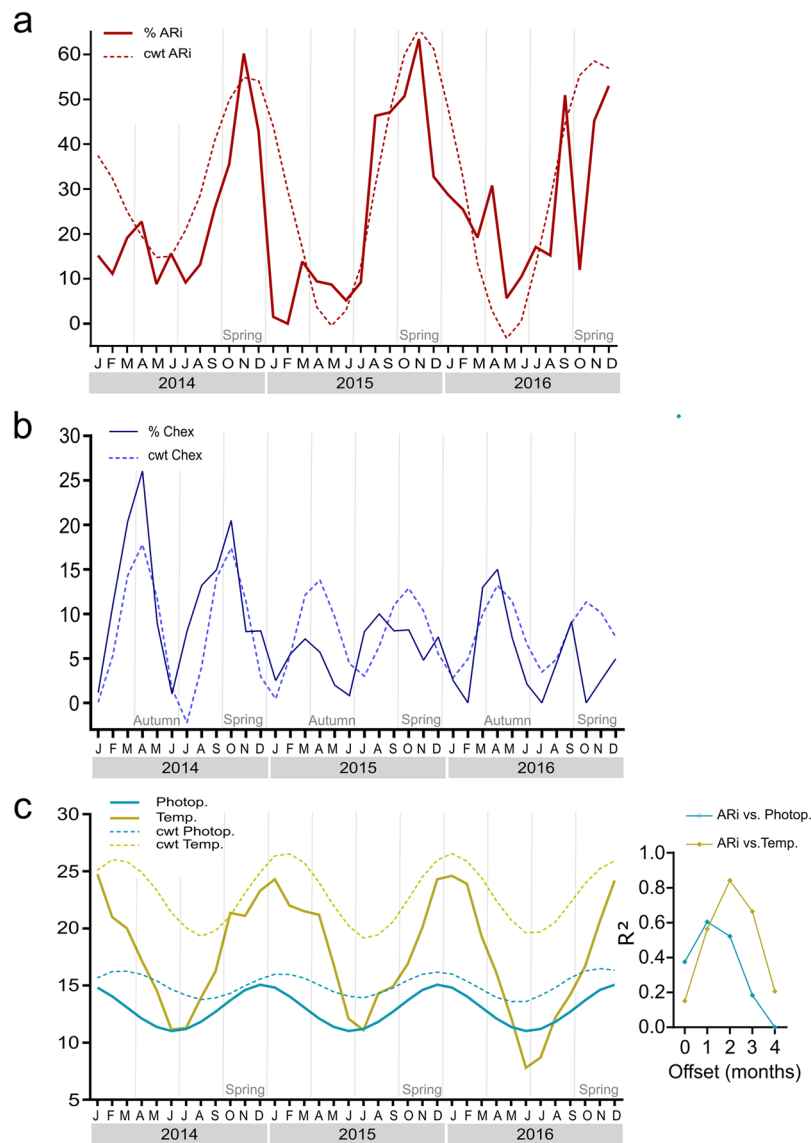


Figure 6. Infradian rhythms observed in sperm physiology after 18 h incubation and its relation to environmental factors. The time series of the % AR_i sperm and the % Chex sperm are shown in panel (a,b), respectively, while photoperiod (light blue) and mean temperature (yellow) time series (continuous lines) are shown in panel (c). The corresponding Morlet Wavelet coefficients (cwt) at different monthly scale (dotted lines) are shown in each panel. Vertical gray lines indicate the change in season. Inset corresponds to the correlation coefficient (R^2) obtained between Morlet Wavelet coefficient at a 12-month scale of % AR_i and photoperiod (blue) or temperature (yellow), at different offsets. To improve visualization, Wavelet coefficients were offset by values of 30, 18, 15 and 10 for % AR_i, temperature, photoperiod, and %Chex, respectively. Data are expressed as the mean of 3–4 independent experiments, for each month, performed with ejaculates from different donors. Temperature and photoperiod are shown as the mean of data from 36 consecutive months. AR_i, induced acrosome reaction; Chex, capacitated spermatozoa recruited by chemotaxis; cwt, wavelet coefficients; Photop., photoperiod; Temp., temperature.

associated with sperm capacitation, such as the intracellular level of calcium and the hyperpolarization of the sperm membrane¹³ increased along incubation but with apparent mild fluctuations.

Interestingly, all the sperm samples incubated for only 2 hours showed negligible capacitation (with % AR_i and % Chex values less than 3%), in contrast to most of the sperm samples that obtained a $\geq 10\%$ level after 18-hour incubation period. Thus, a long incubation ensures that most of the samples acquire the capacitation state, at least in terms of induced acrosome reaction and sperm recruitment by chemotaxis.

Sperm physiology variation may also be associated with an infradian rhythm. Several laboratories investigated seasonality in seminal parameters, since they are a direct consequence of spermatogenesis and epididymis maturation. However, seasonality in sperm concentration, morphology and motility parameters is controversial^{14,18,32}. Here we show that these sperm parameters do not behave with an infradian rhythm.

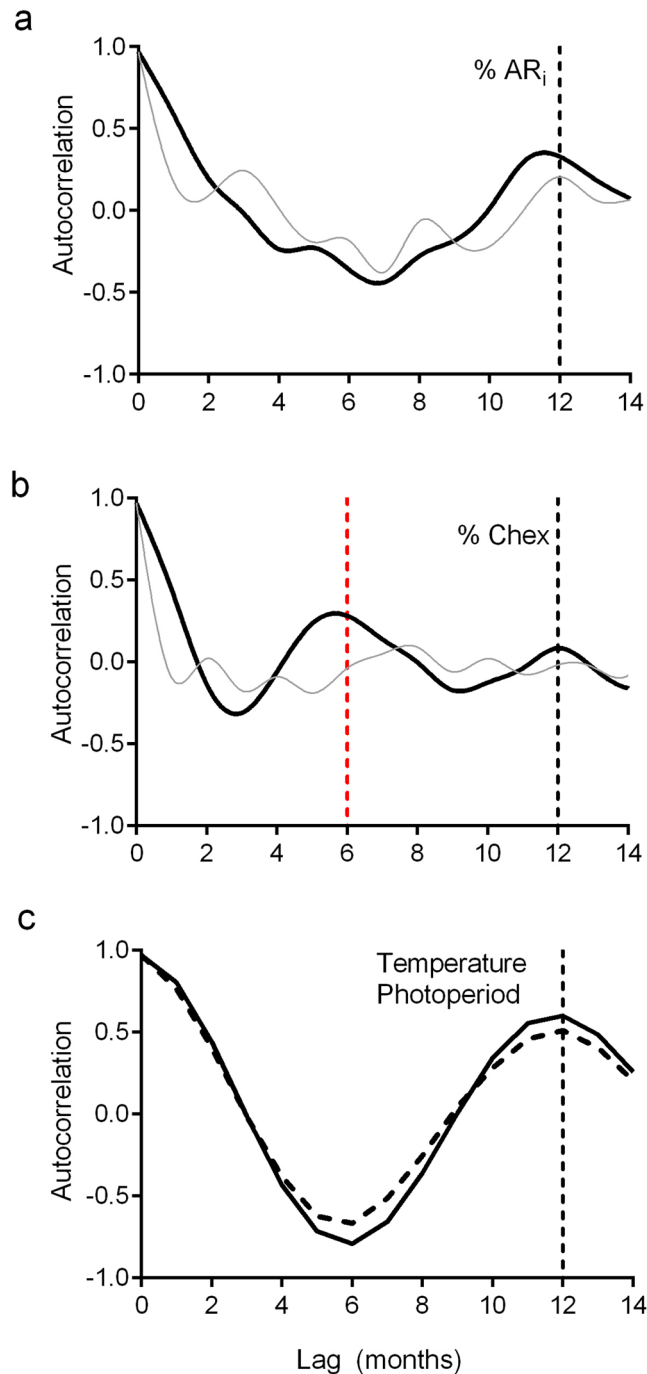


Figure 7. Autocorrelation analysis for sperm capacitation over a 3-year period. Autocorrelation analysis of the % AR_i (a) or % Chex (b) spermatozoa incubated under capacitating conditions for 4 h (gray line) and 18 h (black line), and the average temperature (gray solid line) and photoperiod (dotted line) values (c). Time series used in this analysis are based on data from Fig. 6. Red and black dotted lines highlight the 6 and 12-month cycle, respectively. AR_i, induced acrosome reaction; Chex, capacitated spermatozoa recruited by chemotaxis.

After evaluating sperm capacitation, every month for three years, we concluded that the sperm samples show a different periodicity according to the parameter evaluated. Thus, the % AR_i has a 12-month rhythm with a peak in spring (October–November), meanwhile the % Chex shows a 6-month rhythm, in which, in the first semester of the year, the peak occurs in autumn (March–April), and in the second semester the peak is observed in spring (September–October). The latter matches the peak of the % AR_i and that of meteorological parameters. In other words, the time of the year where the level of capacitation is best is in spring.

Which factors may influence the seasonality observed in sperm physiology? Given that temperature and photoperiod are highly correlated, it is difficult to dissociate their influences on sperm physiology. Moreover, both are quite well correlated to the % AR_i during the year, while the second peak of the year of the % Chex also matches

the increase in meteorological parameters. However, the Chex peak in the first semester of the year seems to be modulated by other unknown factors. The present work shows that the capacitation level is very low in summer and winter; but this may be due to a direct effect of environmental factors on the physiology of spermatozoa or to an indirect effect on spermatogenesis. For instance, the biological influence of photoperiod may reside in that it modulates the seasonal changes in night length, which is negatively correlated with the melatonin concentration in blood^{33–36}. At the cellular level, the biological clock that regulates the cyclicity of somatic cell is governed by the expression of specific genes³⁷. Since the spermatozoon is a transcriptionally inactive cell, another system may operate. For instance, the presence of melatonin in seminal plasma^{38–40} and the corresponding receptors on the sperm surface^{36,39,41} suggest that sperm physiology may be regulated by the melatonin circannual cycle. Indeed, exogenous melatonin administration enhances sperm function and ART results^{42,43}.

Our results show that the circannual rhythm, and in part that of 6 months, may be modulated by the joint action of temperature and photoperiod, while the ultradian rhythm may be influenced by unknown intrinsic sperm factors. Thus, a long incubation (e.g. 18 h) for samples obtained preferably in spring time (in a seasonal climate) would be advisable to avoid false negative results. Here we present an innovative approach to better comprehend human reproductive biology to think experimental designs in the light of sperm cyclicity or to improve sperm aptitude for clinical purposes.

Materials and Methods

Ethics statement. The experiments were performed with human sperm samples provided by volunteer donors. The semen samples were treated in accordance with the Declaration of Helsinki. The study received the approval of the Ethics Committee of the National Clinical Hospital (National University of Cordoba, Argentina; # 061/10) and donors signed an informed consent document.

Reagents and culture medium. All chemicals were purchased from Sigma-Aldrich (St. Lois, MO, USA) unless otherwise indicated. The non-capacitating medium used in this study was modified BWB, containing 120 mM NaCl, 4.8 mM KCl, 0.22 mM CaCl₂, 1.16 mM MgSO₄, 1.16 mM KH₂PO₄, 5 mM Glucose, 0.2 mM Na-Pyruvate, 11.7 mM Na-lactate, 45 mM Hepes, and 8% (w/v) Gentamicin. For capacitating conditions, the medium was supplemented with 25 mM NaHCO₃, 1.68 mM CaCl₂, and 3% (w/v) BSA, and osmolarity was adjusted by reducing the NaCl concentration to 88 mM. All media were adjusted to pH 7.4 and osmolarity was maintained around 290 mOs kg⁻¹.

Sperm preparation. Human sperm samples were collected by masturbation after 2–5 days of sexual abstinence. Only those samples exhibiting normal seminal parameters according to the WHO criteria⁴⁴ were included in the study. Semen samples were liquefied at 37 °C under an atmosphere of 5% CO₂ in air, for 30 min. Then, spermatozoa were separated from the seminal plasma by the migration-sedimentation technique⁴⁵ or the swim-up procedure⁴⁶, as specified in each set of experiments. In both cases, 1 ml of the semen sample was carefully placed beneath 1 ml of BWB capacitating or non-capacitating medium, and then the samples were incubated for 1 h at 37 °C under an atmosphere of 5% CO₂ in air. At the end of incubation, the highly motile sperm population was recovered, and the sperm concentration was adjusted to 6 × 10⁶ sperm/ml in BWB medium, and further incubated with or without capacitation medium for different periods as specified in the Results section.

Sperm capacitation evaluation. Since there is no available marker for sperm capacitation, we used several parameters that indirectly evaluate this physiological state.

Ability of capacitated spermatozoa to undergo the induced acrosome reaction. Briefly, the sperm sample was incubated with or without A23187 calcium ionophore (10 μM) for 30 min at 37 °C¹². Then, the samples were fixed with 2% formaldehyde for 10 min at room temperature, centrifuged at 2000 g and washed twice with 100 mM ammonium acetate at pH 9.0. The pellet was resuspended in 0.2 ml of 100 mM ammonium acetate and 30 μl of the sperm suspension was smeared on a glass slide with the help of another glass slide. The sperm samples were let dry in air and then were incubated in freshly-made Coomassie Brilliant Blue stain (0.22% Coomassie G-250, 50% methanol, 10% glacial acetic acid, and 40% water), for 7 min at room temperature. Slides were thoroughly washed with distilled water to remove excess stain. After air drying, the status of the acrosome (intact or reacted) was evaluated in 200 cells, under bright field microscopy at 100× (*Olympus BX 50*, Center Valley, USA). The percentage of net induced acrosome-reacted spermatozoa (% AR_i) was determined as the difference in the percentages of induced and spontaneous acrosome-reacted spermatozoa.

Recruitment of capacitated spermatozoa by chemotaxis. We applied the Sperm Selection Assay (SSA) device²⁵, which consists of two wells, in which the sperm suspension is placed in one well (W1) and the attractant solution (or culture medium as negative control) in the other (W2). These two wells are connected by a tube, through which the attractant diffuses from W2 to W1, forming a concentration gradient which stimulates sperm chemotaxis. A 10 pM solution of progesterone was used as attractant⁴⁷. The device was then incubated at 37 °C in an atmosphere containing 5% CO₂ in air, for 20 min. At the end of the assay, the net percentage of sperm accumulation in W2 after the SSA (% Chex) was determined. This parameter was calculated as the difference in the percentages of spermatozoa recovered from W2 with or without progesterone.

Protein tyrosine phosphorylation pattern associated with the capacitation state. This parameter was determined with an imaging flow cytometer⁴⁸. The samples were centrifuged at 2000 g for 3 min and the pellet was resuspended in 1 ml of PBS, adjusting the cell concentration to 10 × 10⁶ sperm/ml. Spermatozoa were fixed with 2% (v/v) paraformaldehyde in PBS for 20 min at room temperature, washed, and treated with 0.05% Triton X-100 in

PBS for 15 min. Samples were then centrifuged at 4000 g in PBS for 5 min. The sperm pellet was resuspended in 1 ml of blocking solution (3% BSA in PBS) for 2 h at room temperature. The incubation with the first antibody (anti-phosphotyrosine monoclonal antibody clone 4G10, cat #05–321 from EMD Millipore, 1:500 dilution) was performed in 0.05% (v/v) Tween 20 in PBS (PBS-T), supplemented with 3% BSA, at 4 °C overnight. The sample was then centrifuged at 4000 g in PBS for 5 min and incubated with Alexa-488 conjugated anti-mouse IgG antibody (1:500) diluted in PBS-T, supplemented with 3% BSA, in the dark for 1 h at room temperature, performing the final wash with PBS. The control samples were processed as described above, but lacking either the specific or the second antibody, or both. The protein tyrosine phosphorylation labeling was determined in the sperm tail using an Image-based flow cytometer⁴⁸. Briefly, the mask-based analysis allowed us to identify and quantify pY staining in the different sperm regions using an unbiased approach by quantifying pixel values. We applied the masks to all images and obtained fluorescence intensity values for the principal piece region of every cell (~2000 cells per experiment). Since fluorescence intensity varies among experiments, the comparison between treatments was performed by normalizing each group to the non-capacitating condition, performing the analysis with the percentage of spermatozoa exceeding the third quartile of fluorescence intensity.

Sperm parameters associated with capacitation. Since a variation in the level of intracellular calcium and the membrane potential was observed during sperm capacitation¹³, these two parameters were also studied during incubation, and sperm viability was determined as an internal control.

Sperm intracellular calcium concentration, membrane potential and viability. These parameters were determined by flow cytometry, as previously described by Lopez-Gonzalez *et al.*¹³. Briefly, the sperm plasma membrane potential and $[Ca^{2+}]_i$ changes were monitored using the fluorescent indicators DiSC3(5) and Fluo3-AM, respectively. After incubation under either non-capacitating or capacitating conditions, samples were centrifuged at 750 g for 5 min. Spermatozoa were resuspended in BWW medium and the concentration was adjusted to 4×10^6 sperm/ml. The sperm were loaded with 50 nM DiSC3(5) and 0.5 mM Fluo3-AM during 30 min at 37 °C under 5% CO₂ in air, and after that the spermatozoa were washed by centrifugation. For each experimental condition, 500 µl of the cell suspension were placed in a cytometer tube, and 100 nM propidium iodide (PI) was used to determine sperm viability, added 1 min before collecting data.

Data were recorded as individual cellular events using a FACS Canto IITM cytometer (Becton Dickinson). Forward scatter (FSC) and side scatter (SSC) fluorescence data were collected from 20000 events per sample. Appropriate cytometer settings were selected for DiSC3(5), Fluo3-AM and PI. Threshold levels for FSC and SSC were set to exclude signals from cellular debris. DiSC3(5), Fluo3-AM and PI were excited using a 488-nm argon excitation laser. Nonviable cells became PI positive, and their red fluorescent signal detected as fluorescence of wavelength 670 nm. DiSBAC2(3)-positive cells were detected at 561–606 nm and Fluo3-AM-positive cells were detected at 515–545 nm. Unstained control samples were used to verify that threshold settings were appropriate and to create the corresponding gates needed to discriminate debris from cells. As a positive control, PI-stained dead sperm (sperm suspended in 0.1% Triton X-100 in BWW and incubated 10 min at room temperature) was run in parallel. Data were analyzed using FACS Diva and FlowJo software (Tree Star 9.3.3). The analysis was performed with the percentage of spermatozoa exceeding the third quartile of fluorescence intensity.

Sperm motility. The percentage of motile spermatozoa was determined at the end of each incubation period by means of video microscopy and image analysis⁴⁹, using a phase contrast microscope (Nikon Instruments Inc, NY, USA) and NIS elements software (4.30.01 DU1). The sperm movement from three different fields selected at random was digitally recorded at 30 Hz for 10 s under a 10x objective. Sperm tracks were analyzed by FIJI software using the motility tool plug-in, determining the percentage of motile cells based on motility of at least 200 spermatozoa.

Sperm parameters database provided by a local andrology lab. Data from 4044 normospermic samples, corresponding to sperm concentration, motility and morphology, were determined by standard procedures according to WHO criteria⁴⁴, and collected during three consecutive years (2014–2016) in a local Andrology lab, the standard quality of its procedures is certified by the Argentine Society for Reproductive Medicine.

Meteorological data. The average temperature and the photoperiod were obtained from the meteorological station of the INTA Manfredi (Instituto Nacional de Tecnología Agropecuaria Manfredi, Córdoba, Argentina) for 31°49' South latitude; 63°46' West Length, a 292 masl), which is located 60 km SE from Córdoba city (<https://inta.gob.ar/documentos/informacion-meteorologica-mensual-de-la-eea-manfredi>).

Data analysis to verify periodicity in biological and meteorological parameters. Two different mathematical approaches (autocorrelation and wavelet analysis) were applied) to detect periodicity and precise evolution time in sperm physiology variations.

Autocorrelation. This math analysis generates correlation coefficients for the time series between the biological data and itself as it is sequentially 'lagged' out of phase, one time unit at a time. An autocorrelation function $C(s)$ is estimated between two points in time with a determined lag (s), meaning that data from the same variable at a given time are correlated with data from the same variable taken at a later time. A periodic behavior is distinguished from a random one according to the correlation coefficients robustness and the shape of the curve^{50,51}. Thus, recurring peaks in the correlation curve (meaning positive values followed by negative values and again by a positive one) indicate that the signal is periodic. Conversely, a random behavior (linear stochastic processes) is

also detected by the autocorrelation function, which is represented by an exponential decay exhibiting correlation coefficients approximating to zero. Data analysis was performed using MATLAB R2017a.

Wavelet analysis. This analytical approach consists in a mathematical transformation of a time series of biological data according to a complex mathematical function, which provides information simultaneously on the presence of periodic behavior and its time localization^{52–55}. Wavelet complex analysis expresses a signal (in this case a time series) as a sum of its component waveforms (real and imaginary parts) (Supplementary Fig. S6). Here, the continuous wavelet transform function coefficient (*cwt*) of the time series is represented by their real part (dotted line in Fig. 6 and Supplementary Fig. 6). In the process of analysis, this wavelet is rescaled for each time scale (period) evaluated (“Y” axis in Supplementary Fig. S5). Here we used two complex wavelet functions, the Morlet and the Gaussian. Data analysis in this article was performed using the wavelet toolbox of MATLAB R2017a, in particular the continuous wavelet transform function. The complex Morlet wavelet, *cmor1–1.5*, was used with scales that ranged from 0.3 to 30, corresponding to periods of 0.2 to 20 months^{55,56}. The complex Gaussian wavelet function (*cgau1*), was used with scales that ranged from 0.03 to 6, corresponding to periods of 0.02 to 20 months. For convenience, scales were transformed into frequencies using the *scales2freq* function of MATLAB. The developed script is publicly available⁵⁷. For visualization of synchronicity, we followed Pering *et al.*⁵⁴ using the real part of the *cwt* (*Re(cwt)*), in which the Spearman correlation between *Re(cwt)* of the different signals is evaluated at a given time scale (for review see Kurz *et al.*, 2017)⁵⁸.

Statistical analysis. Data were expressed as the mean \pm SEM of three to ten independent experiments. Differences between treatments were determined by means of one-way ANOVA, and a posteriori Tukey test performed with the Graph Pad Prism 6.01 (La Jolla, CA, USA) unless otherwise indicated, considering statistically significant differences at a level of confidence of 0.05. Cytometry data were analyzed automatically using FACS Diva and FlowJo software and the statistical analysis was performed using the RStudio software, v1.0143⁵⁹. All data were verified to satisfy the parametric assumptions of homogeneity of variances and normality. Statistical approach for time series analysis is described in the previous section.

References

- Barroso, G. *et al.* Developmental sperm contributions: fertilization and beyond. *Fertil. Steril.* **92**, 835–848 (2009).
- Chang, M. Fertilizing Capacity of Spermatozoa deposited into the Fallopian Tubes. *Nature* **168** (1951).
- Austin, C. Observations on the Penetration of the Sperm into the Mammalian Egg. *Australian journal of scientific research. Ser. B: Biological sciences* **4** (1951).
- Zeng, Y., Oberdorf, J. A. & Florman, H. M. pH Regulation in Mouse Sperm: Identification of Na⁺, Cl[–], and [formula] Dependent and Arylamino benzoate-Dependent Regulatory Mechanisms and Characterization of Their Roles in Sperm Capacitation. *Dev. Biol.* **173**, 510–520 (1996).
- Nakanishi, T., Ikawa, M., Yamada, S., Toshimori, K. & Okabe, M. Alkalinization of Acrosome Measured by GFP as a pH Indicator and Its Relation to Sperm Capacitation. *Dev. Biol.* **237**, 222–231 (2001).
- Darszon, A., Guerrero, A., Galindo, B. E., Nishigaki, T. & Wood, C. D. Sperm-activating peptides in the regulation of ion fluxes, signal transduction and motility. *Int. J. Dev. Biol.* **52**, 595–606 (2008).
- de Lamirande, E. & Gagnon, C. Capacitation-associated production of superoxide anion by human spermatozoa. *Free Radical Biology and Medicine* **18**, 487–495 (1995).
- Visconti, P. E., Krapf, D., de la Vega-Beltrán, J. L., Acevedo, J. J. & Darszon, A. Ion channels, phosphorylation and mammalian sperm capacitation. *Asian J. Androl.* **13**, 395–405 (2011).
- Buffone, M. G. *Sperm Acrosome Biogenesis and Function During Fertilization.* **220** (2016).
- Eisenbach, M. & Giojalas, L. C. Sperm guidance in mammals—an unpaved road to the egg. *Nat. Rev. Mol. Cell Biol.* **7**, 276–285 (2006).
- Giojalas, L. C., Guidobaldi, H. A. & Sánchez, R. Sperm Chemotaxis in Mammals. *Flagellar Mech. Sperm Guid.* 272–307 (2015).
- Jaiswal, B. S., Cohen-Dayag, A., Tur-Kaspa, I. & Eisenbach, M. Sperm capacitation is, after all, a prerequisite for both partial and complete acrosome reaction. *FEBS Lett.* **427**, 309–313 (1998).
- López-González, I. *et al.* Membrane hyperpolarization during human sperm capacitation. *Mol. Hum. Reprod.* **20**, 619–629 (2014).
- Centola, G. M. & Eberly, S. Seasonal variations and age-related changes in human sperm count, motility, motion parameters, morphology, and white blood cell concentration. *Fertil. Steril.* **72**, 803–808 (1999).
- Krause, A. & Krause, W. Seasonal variations in human seminal parameters. *Eur. J. Obstet. Gynecol. Reprod. Biol.* **101**, 175–178 (2002).
- Pol, P. S., Beuscart, R., Leroy-Martin, B., Hermand, E. & Jablonski, W. Circannual rhythms of sperm parameters of fertile men*. *Fertil. Steril.* **51**, 1030–1033 (1989).
- Gyllenberg, J., Skakkebaek, N. E., Nielsen, N. C., Keiding, N. & Giwercman, A. Secular and seasonal changes in semen quality among young Danish men: a statistical analysis of semen samples from 1927 donor candidates during 1977–1995. *Int. J. Androl.* **22**, 28–36 (1999).
- Mao, H., Feng, L. & Yang, W.-X. Environmental factors contributed to circannual rhythm of semen quality. *Chronobiol. Int.* **34**, 411–425 (2017).
- Ombelet, W. *et al.* Chronobiological fluctuations in semen parameters with a constant abstinence period. *Arch Androl* **37**, 91–96 (1996).
- Chia, S.-E., Lim, S.-T. A., Ho, L.-M. & Tay, S.-K. Monthly variation in human semen quality in male partners of infertile women in the tropics. *Hum. Reprod.* **16**, 277–281 (2001).
- Malm, G. *et al.* Reproductive Function during Summer and Winter in Norwegian Men Living North and South of the Arctic Circle. *J. Clin. Endocrinol. Metab.* **89**, 4397–4402 (2004).
- Lewis, S. E. M. Is sperm evaluation useful in predicting human fertility? *Reproduction* **134**, 31–40 (2007).
- Barratt, C. L. R., Mansell, S., Beaton, C., Tardif, S. & Oxenham, S. K. Diagnostic tools in male infertility—the question of sperm dysfunction. *Asian J. Androl.* **13**, 53–58 (2011).
- Cazelles, B., Chavez, M., Constantin De Magny, G., Guégan, J.-F. & Hales, S. Time-dependent spectral analysis of epidemiological time-series with wavelets. *J. R. Soc. Interface* **4**, 625–636 (2007).
- Gatica, L. V. *et al.* Picomolar gradients of progesterone select functional human sperm even in subfertile samples. *Mol. Hum. Reprod.* **19**, 559–569 (2013).
- Cohen-Dayag, A., Tur-Kaspa, I., Dor, J., Mashiach, S. & Eisenbach, M. Sperm capacitation in humans is transient and correlates with chemotactic responsiveness to follicular factors. *Proc. Natl Acad. Sci. USA* **92**, 11039–11043 (1995).

27. Fabro, G. *et al.* Chemotaxis of capacitated rabbit spermatozoa to follicular fluid revealed by a novel directionality-based assay. *Biol. Reprod.* **67**, 1565–1571 (2002).
28. Oren-Benaroya, R., Kipnis, J. & Eisenbach, M. Phagocytosis of human post-capacitated spermatozoa by macrophages. *Hum. Reprod.* **22**, 2947–2955 (2007).
29. Uñates, D. R. *et al.* Versatile action of picomolar gradients of progesterone on different sperm subpopulations. *Plos One* **9**, e91181 (2014).
30. Eisenbach, M. & Giojalas, L. C. Sperm guidance in mammals — an unpaved road to the egg. *Nat Rev Mol Cell Biol* **7**, 276–285 (2006).
31. Guidobaldi, H. A., Hirohashi, N., Cubilla, M., Buffone, M. G. & Giojalas, L. C. An intact acrosome is required for the chemotactic response to progesterone in mouse spermatozoa. *Mol. Reprod. Dev.* **84**, 310–315 (2017).
32. Levine, R. J. Seasonal variation of semen quality and fertility. *Scand. J. Work. Environ. Health* **25**, 34–37 (1999).
33. Wehr, T. A. Melatonin and Seasonal Rhythms. *J. Biol. Rhythms* **12**, 518–527 (1997).
34. Morera, A. L. & Abreu, P. Seasonality of psychopathology and circannual melatonin rhythm. *J. Pineal Res.* **41**, 279–283 (2006).
35. Reiter, R. J. The melatonin rhythm: both a clock and a calendar. *Experientia* **49**, 654–664 (1993).
36. Ortiz, A. *et al.* High endogenous melatonin concentrations enhance sperm quality and short-term *in vitro* exposure to melatonin improves aspects of sperm motility. *J. Pineal Res.* **50**, 132–139 (2011).
37. Xue, T., Song, C., Wang, Q., Wang, Y. & Chen, G. Investigations of the CLOCK and BMAL1 Proteins Binding to DNA: A Molecular Dynamics Simulation Study. *PLoS One* **11**, e0155105 (2016).
38. Luboshitzky, R., Shen-Orr, Z. & Herer, P. Seminal plasma melatonin and gonadal steroids concentrations in normal men. *Arch Androl.* **48**, 225–32 (2002).
39. González-Arto, M. *et al.* Melatonin receptors MT1 and MT2 are expressed in spermatozoa from several seasonal and nonseasonal breeder species. *Theriogenology* **86**, 1958–1968 (2016).
40. Awad, H., Halawa, F., Mostafa, T. & Atta, H. Melatonin hormone profile in infertile males. *Int. J. Androl.* **29**, 409–413 (2006).
41. Dubocovich, M. L. & Markowska, M. Functional MT1 and MT2 melatonin receptors in mammals. *Endocrine* **27**, 101–110 (2005).
42. Sharbatoghli, M., Rezazadeh Valojerdi, M., Bahadori, M. H., Salman Yazdi, R. & Ghaleno, L. R. The Relationship between Seminal Melatonin with Sperm Parameters, DNA Fragmentation and Nuclear Maturity in Intra-Cytoplasmic Sperm Injection Candidates. *Cell J.* **17**, 547–553 (2015).
43. Cruz, M. H. C., Leal, C. L. V., Cruz, J. F. da, Tan, D. X. & Reiter, R. J. Role of melatonin on production and preservation of gametes and embryos: A brief review. *Anim. Reprod. Sci.* **145**, 150–160 (2014).
44. World Health Organization. *WHO laboratory manual for the examination and processing of human semen, 5th edn.* Geneva, Switzerland: WHO Press, 2010. (2010).
45. Sánchez, R., Risopatrón, J., Sepúlveda, G., Peña, P. & Miska, W. Evaluation of the acrosomal membrane in bovine spermatozoa: Effects of proteinase inhibitors. *Theriogenology* **43**, 761–768 (1995).
46. Mata-Martínez, E. *et al.* Measuring Intracellular Ca²⁺ Changes in Human Sperm using Four Techniques: Conventional Fluorometry, Stopped Flow Fluorometry, Flow Cytometry and Single Cell Imaging. *J. Vis. Exp.* e50344 (2013).
47. Teves, M. E. *et al.* Progesterone at the picomolar range is a chemoattractant for mammalian spermatozoa. *Fertil. Steril.* **86**, 745–749 (2006).
48. Matamoros-Volante, A. *et al.* Semi-automatized segmentation method using image-based flow cytometry to study sperm physiology: the case of capacitation-induced tyrosine phosphorylation. *Mol Hum Reprod.* **2**, 64–73 (2018).
49. Guidobaldi, H. A., Teves, M. E., Uñates, D. R., Anastasia, A. & Giojalas, L. C. Progesterone from the Cumulus Cells Is the Sperm Chemoattractant Secreted by the Rabbit Oocyte Cumulus Complex. *PLoS One* **3**, e3040 (2008).
50. Dowse, H. B. Chapter 6 Analyses for Physiological and Behavioral Rhythmicity. In *Computer Methods, Part A* **454**, 141–174 (2009).
51. Mourão, M., Satin, L. & Schnell, S. Optimal Experimental Design to Estimate Statistically Significant Periods of Oscillations in Time Course Data. *PLoS One* **9**, e93826 (2014).
52. Leise, T. L. Wavelet analysis of circadian and ultradian behavioral rhythms. *J. Circadian Rhythms* **11**, 5 (2013).
53. Ghosh, S., Manimaran, P. & Panigrahi, P. K. Characterizing multi-scale self-similar behavior and non-statistical properties of fluctuations in financial time series. *Phys. A Stat. Mech. its Appl.* **390**, 4304–4316 (2011).
54. Pering, T. D., Tamburello, G., McGonigle, A. J. S., Hanna, E. & Aiuppa, A. Correlation of oscillatory behaviour in Matlab using wavelets. *Comput. Geosci.* **70**, 206–212 (2014).
55. Guzmán, D. A. *et al.* The fractal organization of ultradian rhythms in avian behavior. *Sci. Rep.* **7**, 684 (2017).
56. Gerkema, M. P., Groos, G. A. & Daan, S. Differential Elimination of Circadian and Ultradian Rhythmicity by Hypothalamic Lesions in the Common Vole, *Microtus arvalis*. *J. Biol. Rhythms* **5**, 81–95 (1990).
57. Kembro, J. M. & Flesia, A. G. Wavelet analysis for behavioral time series Title. *FigShare* (2015).
58. Kurz, F. T. *et al.* Network dynamics: quantitative analysis of complex behavior in metabolism, organelles, and cells, from experiments to models and back. *Wiley Interdiscip. Rev. Syst. Biol. Med.* **9**, e1352 (2017).
59. R Core Team. R: A Language and Environment for Statistical Computing (2017).

Acknowledgements

The authors thank Paulina Torres-Rodriguez for her help and technical assistance with the flow cytometer, and Victoria Molina and Marisa Cubilla for their assistance at the beginning of the study. J.M.K., L.C.G. and H.A.G. are researchers of the Consejo Nacional de Investigaciones Científicas y Técnicas. This study was supported by Secyt-UNC-PID “A”-2016–2017, and by DGAPA (IN203116 to C. Treviño), Fronteras-CONACyT N° 71.

Author Contributions

A.M.I. performed experiments, analyzed data and wrote the article; J.M.K. analyzed time series data and revised the article; E.M.D., M.N.G. and A.M.V. performed experiments; R.M. provided data from the Andrology lab; H.A.G., M.J.F., A.B., N.A.P. and C.A.N.M. revise the article; C.L.T. got financial support and revised article L.C.G. designed the study and experiments, got financial support, wrote the article.

Additional Information

Supplementary information accompanies this paper at <https://doi.org/10.1038/s41598-019-42430-4>.

Competing Interests: A.M-I., J.M.K., E.M.D., A.M.V., M.N.G., R.M., C.L.T., M.J.F., A.B., N.A.P. and C.A.N.M. declare not competing interests. L.C.G. and H.A.G. are inventors of the SSA device, and the Consejo de Investigaciones Científicas y Técnicas and the Universidad Nacional de Córdoba are the owners of the patent.

Publisher’s note: Springer Nature remains neutral with regard to jurisdictional claims in published maps and institutional affiliations.



Open Access This article is licensed under a Creative Commons Attribution 4.0 International License, which permits use, sharing, adaptation, distribution and reproduction in any medium or format, as long as you give appropriate credit to the original author(s) and the source, provide a link to the Creative Commons license, and indicate if changes were made. The images or other third party material in this article are included in the article's Creative Commons license, unless indicated otherwise in a credit line to the material. If material is not included in the article's Creative Commons license and your intended use is not permitted by statutory regulation or exceeds the permitted use, you will need to obtain permission directly from the copyright holder. To view a copy of this license, visit <http://creativecommons.org/licenses/by/4.0/>.

© The Author(s) 2019